

Electrochemical characterization of the Poly(2, 2'-Bithiophene-co-Pyrene) Functionalized Single-Walled Carbon Nanotubes Films and Their Applications in Supercapacitors Field

M. Baibarac*, I. Baltog and M. Daescu

National Institute of Materials Physics, Lab. Optical Processes in Nanostructured Materials, P.O. Box MG-7, Bucharest, R077125, Romania

*E-mail: barac@infim.ro

Received: 14 December 2016 / Accepted: 22 January 2017 / Published: 12 February 2017

The performance of the poly(2, 2'-bithiophene-co-pyrene) copolymer doped with bis(2-ethyl hexyl) sulfosuccinate sodium (AOT) anions [(PBTh-Py)⁺AOT⁻] and its composite with single-walled carbon nanotubes (SWNTs) [(PBTh-Py)⁺AOT⁻/SWNTs] as active materials for the electrodes of symmetrical supercapacitors is demonstrated in this work. Using cyclic voltammetry, the influence of the electrolyte concentration and the different cations on the oxidation and reduction processes at the electrolyte/electrode interface is reported. Using charge-discharge galvanostatic measurements in the case of the symmetrical-supercapacitors having as electrode active materials, the (PBTh-Py)⁺AOT⁻ copolymer and the (PBTh-Py)⁺AOT⁻/SWNTs composite, values of the specific capacitance equal with 11.5 and 59 F g⁻¹, respectively, for current densities of 100 mA g⁻¹, were reported.

Keywords: carbon nanotubes, copolymers, cyclic voltammetry

1. INTRODUCTION

The interest for the composites based on poly(2, 2'-bithiophene-co-pyrene) (PBTh-Py) copolymer and single-walled carbon nanotubes (SWNTs) dates from 2014. [1] Until now, two methods were used to synthesis of this composite material, i.e. electrochemical [2] and chemical polymerization. [1] Using surface enhanced Raman scattering and FTIR spectroscopy, it was demonstrated that the chemical polymerization of 2, 2'-bithiophene and pyrene in the presence of SWNTs results in a covalent functionalization of SWNTs with PBTh-Py copolymer in doped state. [1] In the case of the electrochemical polymerization of 2, 2'-bithiophene and pyrene in the presence of SWNTs, the reaction product resulted corresponds SWNTs covalently functionalized with PBTh-Py copolymer in a partially doped state. [2] Several properties of these composite materials reported until

now were: i) the quenching process of the PBTh-Py photoluminescence in the presence of SWNTs, which was explained to have origin both from an energy transfer and a charge collecting mechanism; [1] ii) the preferential orientation of the PBTh-Py/SWNTs composite onto Au support assess from the change of the FTIR spectra under *s*- and *p*-polarized light; [1,2] and iii) an abnormal anti-Stokes Raman scattering process highlighted on the PBTh-Py copolymer and the PBTh-Py/SWNTs composite, which has been explained as resulting from non-linear optical properties induced of macromolecular compound under resonant optical excitation. [2]

Despite significant effort devoted to use of conducting polymers and their composites with various carbon nanoparticles in the energy storage, a little attention has been given to use of composites of the type copolymers/carbon particles in the supercapacitor field. In fact, the interest in the use of copolymers in the supercapacitors field is dated 2009, when were reported values of specific capacitance of electrodes based on poly(pyrrole-co-aniline) equal with 827 F g^{-1} at the currents of 8 mA cm^{-2} in the electrolytes of the type $1 \text{ mol l}^{-1} \text{ Na}_2\text{SO}_4$. [3] Other copolymers used as active material in the supercapacitors field were those having repeating units based on pyrrole and 3-(4-tert-butylphenyl)thiophene [4] and pyrrole formyl pyrrole. [5] Beginning with 2015, a special attention was given to composite materials based on copolymers and carbon particles as electrode materials for supercapacitors. [5,6] Several examples concerning the progress recorded in this field are: i) Liang's work which reports the values of the specific capacitance of electrodes based on reduced graphene oxide and poly(aniline-co-pyrrole) equal with 541 F g^{-1} at the scan rate of 1 mV s^{-1} in Na_2SO_4 electrolyte; [5] and ii) the Gholami's paper, when the best specific capacitance was reported to be equal with 220.3 mF cm^{-2} for pyrrole formyl pyrrole copolymer coated on carbon microfibers at discharge charge of $3 \times 10^{-4} \text{ A}$. [6] After the best knowledge of the authors, at present there is not an article which to invoke the use of composite material based on the (PBTh-Py) copolymer and SWNTs in the energy storage field. Therefore, in this work, we will show that the composite based on the PBTh-Py copolymer and SWNTs can be used as active material for the electrodes of symmetrical supercapacitors.

2. EXPERIMENTAL

Chemical compounds used in this work, i.e. 2, 2'-bithiophene (BTh), pyrene (Py), bis(2-ethyl hexyl) sulfosuccinate sodium (AOT), LiClO_4 , CH_3CN , NaClO_4 , KClO_4 , LiPF_6 , SWNTs, poly(vinylidene fluoride) (PVDF), dibutyl phtalate (DBP), ethylene carbonate (EC), dimethyl carbonate (DMC) and acetone were purchased from Sigma-Aldrich company. Super P conductive carbon black was purchased from TIMCAL-UK.

The electrochemical synthesis of the PBTh-Py copolymer and the PBTh-Py/SWNTs composite has been performed by cyclic voltammetry in the potential range (-1; +1.6) V vs. Ag/AgCl, with a sweep rate of 100 mV s^{-1} applied on the Au plate or Au support covered with a SWNT film. [2] The synthesis solution of the PBTh-Py copolymer or the PBTh-Py/SWNTs composite has consisted of 10^{-2} M BTh, 10^{-2} M Py and 10^{-3} M AOT in CH_3CN . All cyclic voltammograms were stopped at the potential of +1.6 V vs. Ag/AgCl, the reaction products in the absence and in the presence SWNTs

being the PBTh-Py copolymer doped with AOT anions (abbreviated as $(\text{PBTh-Py})^+\text{AOT}^-$) and SWNTs covalently functionalized with PBTh-Py doped with AOT anions (abbreviated as $(\text{PBTh-Py})^+\text{AOT}^-/\text{SWNTs}$). [2] In order to prepare films with the thickness of 33 nm, i) 25 cyclic voltammograms were recorded onto the blank Au electrode in the case of the electrosynthesis of the $(\text{PBTh-Py})^+\text{AOT}^-$ film and ii) 15 cyclic voltammograms were recorded onto the Au electrode covered with a SWNTs layer having the thickness of 12 nm. The cyclic voltammetry was performed using an electrochemical cell with a single-compartment endowed with three electrodes consisting in a working electrode based on a Au plate covered with films of $(\text{PBTh-Py})^+\text{AOT}^-$ or $(\text{PBTh-Py})^+\text{AOT}^-/\text{SWNTs}$, a Pt wire as counter electrode and a reference electrode of the type the Ag/AgCl electrode.

To assess of the performance of the $(\text{PBTh-Py})^+\text{AOT}^-$ copolymer or the $(\text{PBTh-Py})^+\text{AOT}^-/\text{SWNTs}$ composite as active materials for symmetrical-supercapacitor cells, films electrochemical prepared as noted above were peeled off in order to prepare a mixture having 80 wt.% active material, 5 wt.% PVDF as binding, 15 wt.% super-P conductive carbon black, 2 drops of DBP and 1 ml acetone. The protocol for the preparation of electrodes was described in Ref. [7]. The electrolyte used was a 1M LiPF_6 solution in a 50:50 mixture in volume of EC and DMC. The assembled symmetrical supercapacitor cells were cycled between -1.6 and +1.6 V. The assessing of the performance of the $(\text{PBTh-Py})^+\text{AOT}^-$ copolymer or the $(\text{PBTh-Py})^+\text{AOT}^-/\text{SWNTs}$ composite as active materials for symmetrical-supercapacitor cells was carried out by cyclic voltammetry and charge-discharge galvanostatic measurements.

3. RESULTS AND DISCUSSION

Figures 1 and 2 show cyclic voltammograms of the $(\text{PBTh-Py})^+\text{AOT}^-$ copolymer and the $(\text{PBTh-Py})^+\text{AOT}^-/\text{SWNTs}$ composite, when working electrodes were immersed in the different electrolytes as LiClO_4 , NaClO_4 , KClO_4 with the concentration of 0.05 M. Depending on the electrolyte type, in the case of the Au electrode covered with a $(\text{PBTh-Py})^+\text{AOT}^-$ film one observes that the cyclic voltammogram recorded in the presence of the solution of: i) LiClO_4 shows two oxidation maxima peaked at +0.57 and +1.24 V vs. Ag/AgCl and two reduction maxima situated at -0.17 and -0.72 V vs. V vs. Ag/AgCl; ii) NaClO_4 , an oxidation peak at +1.41 V vs. Ag/AgCl and a reduction peak at -0.67 V vs. Ag/AgCl and iii) KClO_4 , an oxidation peak at +0.14 V vs. Ag/AgCl and a reduction peak at -0.63 V vs. Ag/AgCl. These changes can be explained by analogy with the studies reported in the case of other conducting polymers. [8-12] In the potential range (+1.6; -1) V vs. Ag/AgCl the copolymer is reduced and the AOT anions are expelled. In the potential range (-1; +1.6) V, the re-oxidation of the copolymer when the insertion of the anions of electrolyte takes place. The total reaction which characterizes the oxidation and reduction processes that take place at the interface of the electrode Au covered with the copolymer $(\text{PBTh-PY})^+\text{AOT}^-$ and perchlorate salts solution, can be written as follows:



where $\text{X}^+=\text{Li}^+, \text{Na}^+, \text{K}^+$; (PBTh-Py) is the copolymer in the undoped state and $(\text{PBTh-Py})^+$ corresponds to the copolymer in the doped state.

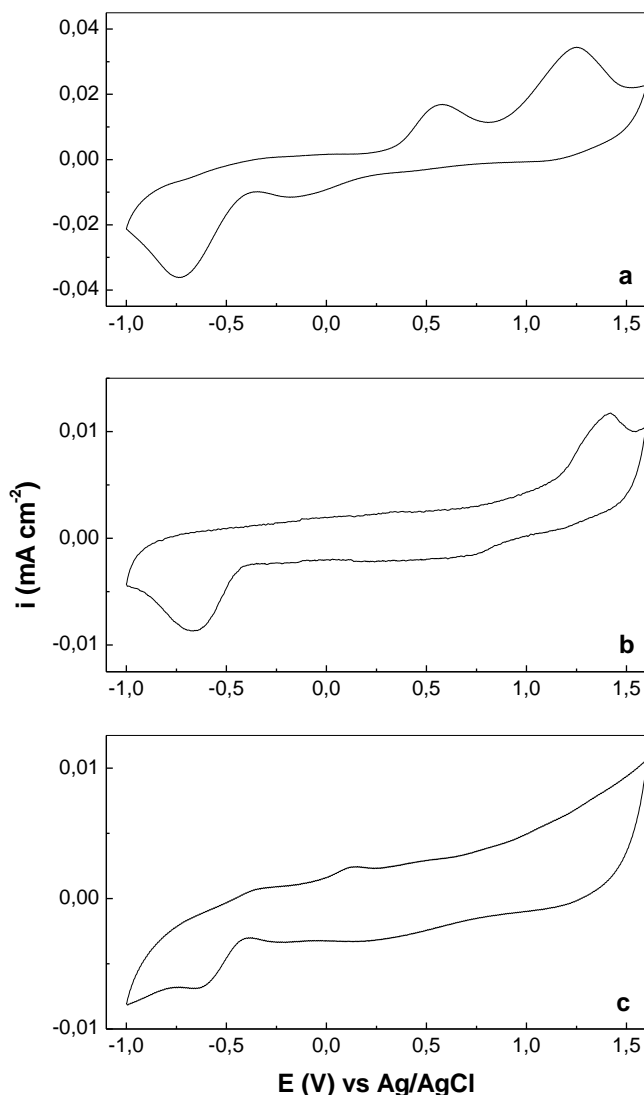
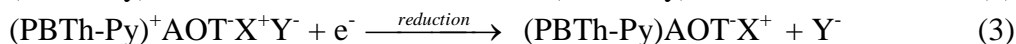
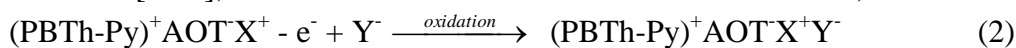


Figure 1. Cyclic voltammograms of the (PBTh-Py)⁺AOT⁻ electrode immersed in the solution of 0.05 M LiClO₄, 0.05 M NaClO₄ and 0.05 M KClO₄ recorded in the potential range (-1; +1.6) V vs. Ag/AgCl with a sweep rate of 100 mV s⁻¹. All figures show the fifth cycle.

Taking into account that AOT anions have a large size, the migration of these anions from and in the copolymer matrix one occurs with difficulty. This fact facilitates the migration of the cations and anions electrolyte with smaller sizes to and from the copolymer matrix. By analogy with the studies reported in Refs. [8-12], the oxidation and reduction reactions in this case, can be written as follows:



where Y⁻ is ClO₄⁻, (PBTh-Py)⁺AOT⁻X⁺Y⁻ is the copolymer in re-oxidized state of the and (PBTh-Py)AOT⁻X⁺ is the copolymer in reduced state.

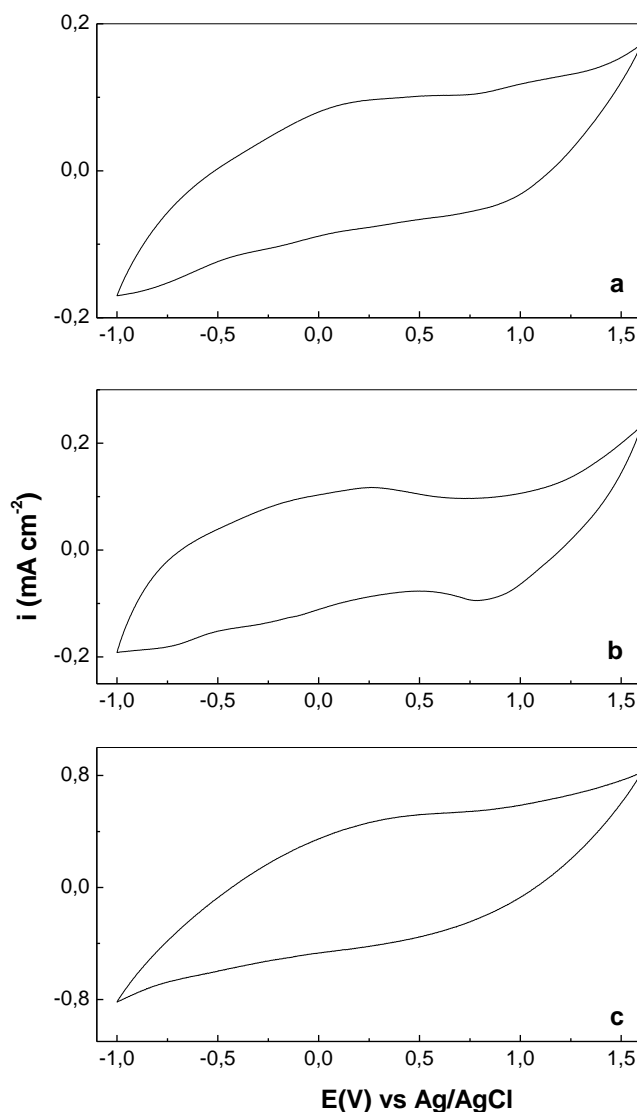


Figure 2. Cyclic voltammograms of the $(\text{PBTh-Py})^+\text{AOT}^-/\text{SWNTs}$ electrode immersed in the solutions of 0.05 M LiClO_4 , 0.05 M NaClO_4 and 0.05 M KClO_4 , recorded in the potential range (-1; +1.6) V vs Ag/AgCl with a sweep rate of 100 mV s^{-1} . All figures show the fifth cycle.

In the case of the $(\text{PBTh-Py})^+\text{AOT}^-/\text{SWNTs}$ composite, the cyclic voltammograms (Fig. 2) show a rectangular profile and higher current densities in comparison with those recorded in the case of the $(\text{PBTh-Py})^+\text{AOT}^-$ copolymer (Fig. 1). This fact indicates that the conducting properties of the composite are superior to those reported in the case of copolymer. A similar behavior was reported for a large range of the composites as polypyrrole/ SWNTs [13], polythiophene/multi-walled carbon nanotubes (MWNTs) [14], poly(o-toluidine)/MWNTs [15], poly(vinylferrocene)/MWNTs [16] and not least polyindole/carbon nanotubes [17]. According to Refs. [13-17], these features originate in the generation of the more active sites on carbon nanotubes surface, as a result of the functionalization of SWNTs with conjugated polymers, and large surface area of carbon nanotubes.

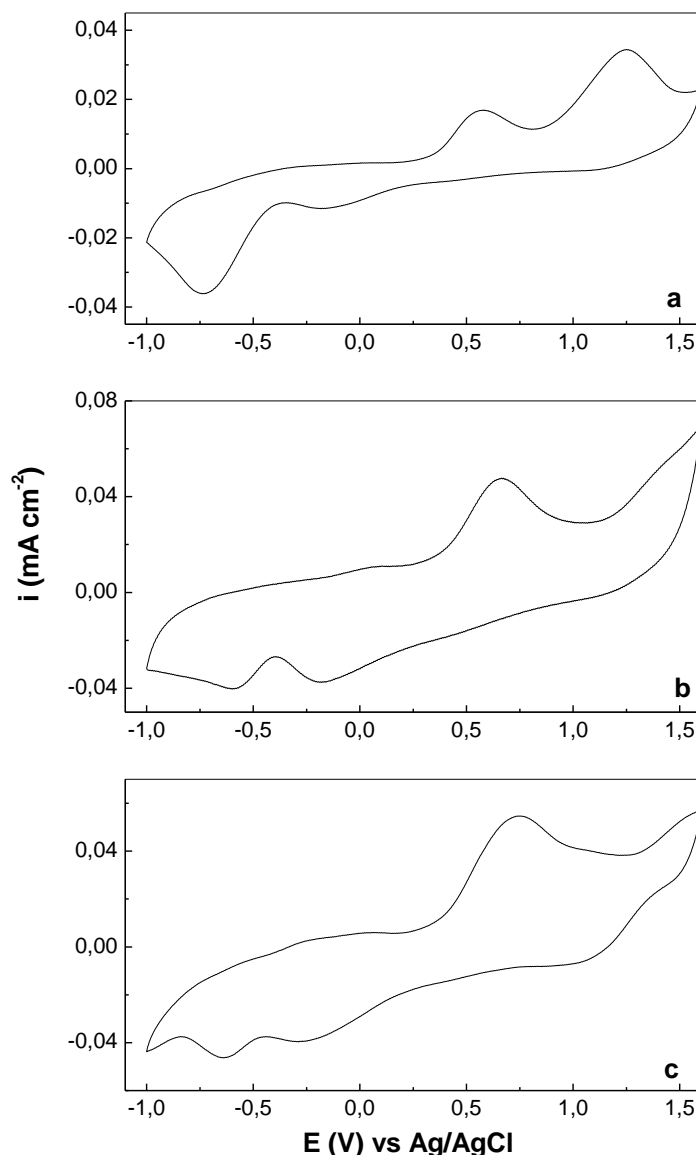


Figure 3. Cyclic voltammograms of the $(\text{PBTh-Py})^+\text{AOT}^-$ electrode immersed in the LiClO_4 solutions with the concentration of 0.05 M, 0.1 M and 0.2 M, recorded in the potential range (-1;+1.6) V vs Ag/AgCl with sweep rate of 100 mV s^{-1} . All figures show the fifth cycle.

Figs. 3 and 4 show the influence of electrolyte concentration on the oxidation and reduction processes at the interfaces electrolyte with electrodes of the type of the $(\text{PBTh-Py})^+\text{AOT}^-$ copolymer and the $(\text{PBTh-Py})^+\text{AOT}^-/\text{SWNTs}$ composite. According to Fig. 3, in the case of the $(\text{PBTh-Py})^+\text{AOT}^-$ copolymer, the increase of the LiClO_4 concentration from 0.05 to 0.2 M leads to: i) an up-shift of oxidation potential from +0.57 to +0.72 V vs. Ag/AgCl simultaneously with a down-shift of the reduction potential from -0.16 to -0.27 V vs. Ag/AgCl and ii) higher anodic/cathodic current densities, whose values in the case of the working electrode immersed in the LiClO_4 solutions with the concentrations of 0.05 and 0.2 M are 0.017 /0.012 mA cm^{-2} and 0.055 /0.039 mA cm^{-2} , respectively. These changes indicate an improvement of the conducting properties of the $(\text{PBTh-Py})^+\text{AOT}^-$ copolymer as increasing the LiClO_4 solution concentration..

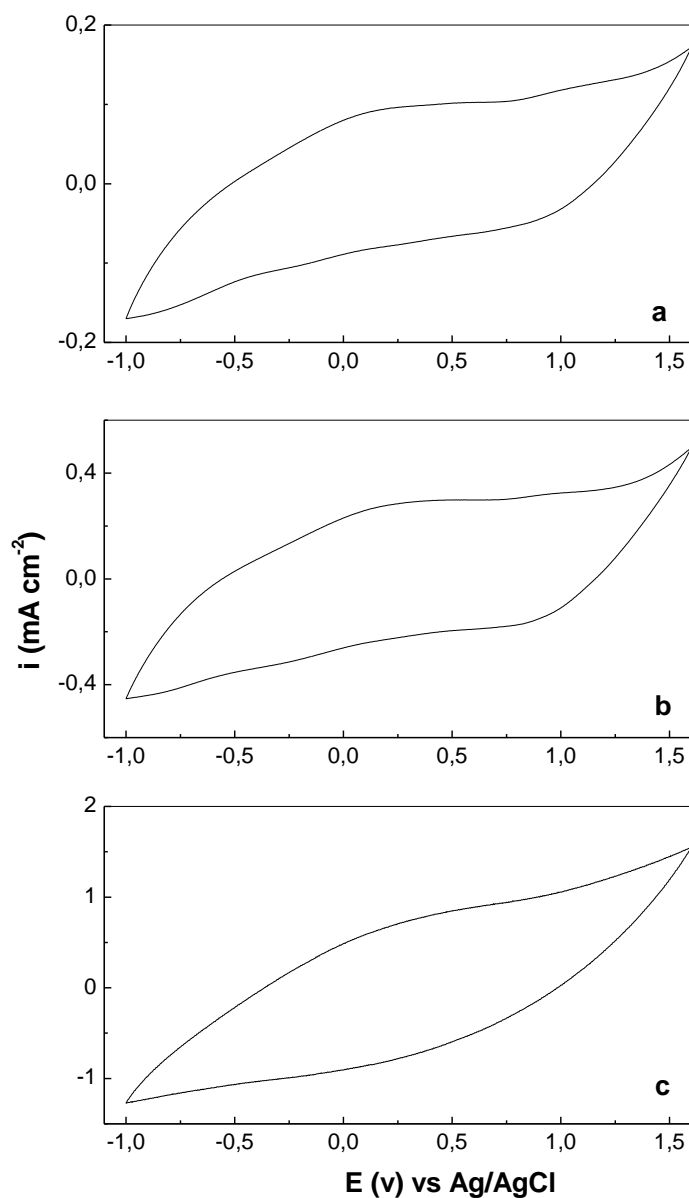


Figure 4. Cyclic voltammograms of the $(\text{PBTh-Py})^+\text{AOT}^-/\text{SWNTs}$ electrode immersed in the LiClO_4 solutions with the concentration of 0.05 M, 0.1 M and 0.2 M, recorded in the potential range (-1; +1.6) V vs. Ag/AgCl with a sweep rate of 100 mV s^{-1} . All figures show the fifth cycle.

Regardless the electrolyte concentration, an increase with one order in magnitude of the anodic and cathode current densities is observed in the case of the cyclic voltammograms recorded when Au electrode covered with the $(\text{PBTh-Py})^+\text{AOT}^-/\text{SWNTs}$ film is immersed in LiClO_4 solution (Fig. 4).

The behavior of the electrodes of Au covered with the films of the $(\text{PBTh-Py})^+\text{AOT}^-$ copolymer and the $(\text{PBTh-Py})^+\text{AOT}^-/\text{SWNTs}$ composites immersed in 0.05 M LiClO_4 solution during recording of 100 cyclic voltammograms is shown in Figs. 5 and 6.

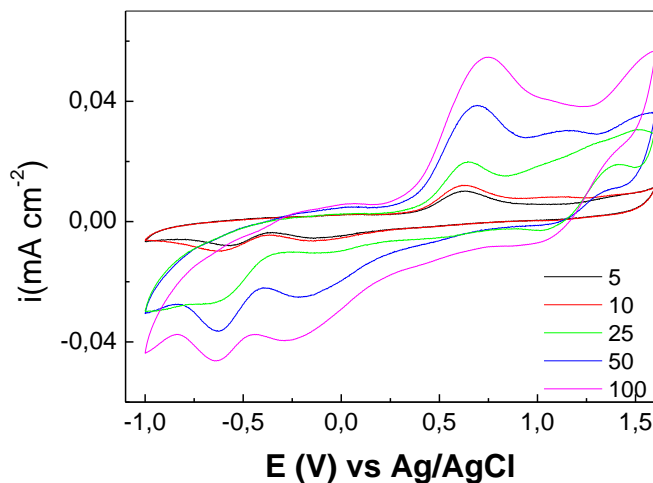


Figure 5. Cyclic voltammograms of the $(\text{PBTh-Py})^+\text{AOT}^-$ electrode immersed in the solution 0.05 M LiClO_4 , recorded in the potential range (-1; +1.6) V vs Ag/AgCl with a sweep rate of 100 mV s^{-1} . The black, red, green, blue and magenta curves correspond to 5th, 10th, 25th, 50th and 100th cyclic voltammograms.

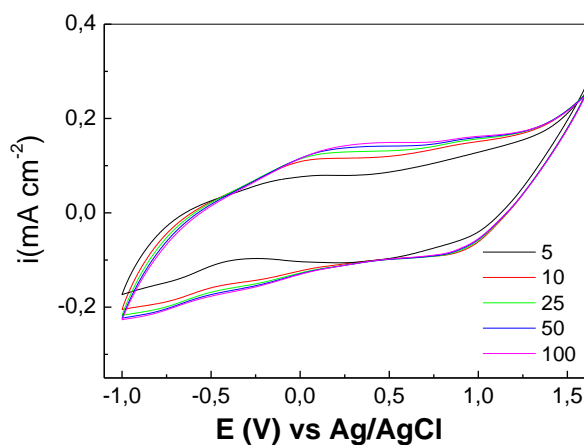


Figure 6. Cyclic voltammograms of the $(\text{PBTh-Py})^+\text{AOT}^-/\text{SWNTs}$ electrode immersed in the solution 0.05 M LiClO_4 , recorded in the potential range (-1; +1.6) V vs Ag/AgCl with a sweep rate of 100 mV s^{-1} . The black, red, green, blue and magenta curves correspond to 5th, 10th, 25th, 50th and 100th cyclic voltammograms

The gradual recording of 100 cyclic voltammograms onto the Au electrodes covered with films of the $(\text{PBTh-Py})^+\text{AOT}^-$ copolymer (Fig. 5) and the $(\text{PBTh-Py})^+\text{AOT}^-/\text{SWNTs}$ composites (Fig. 6) immersed in 0.5M LiClO_4 solution induces: i) an increase in the current density of the anodic and cathodic maxima situated in the potential range (+0.5; +1) V and (-1; 0) V in the case of the $(\text{PBTh-Py})^+\text{AOT}^-$ copolymer (Fig. 5); a similar behavior is highlighted in the case of the Au electrode covered with a film of the $(\text{PBTh-Py})^+\text{AOT}^-/\text{SWNTs}$ composites (Fig. 6); and ii) an up-shift of the anodic peak from +0.63 V to +0.74 V that is accompanied of a down-shift of the cathodic peaks from -0.14 and -

0.56 V to -0.28 and -0.62 V vs. Ag/AgCl, respectively is remarked in the case of the (PBTh-Py)⁺AOT⁻ copolymer (Fig. 5); an up-shift of the anodic peak from +0.1 to +0.35 V vs. Ag/AgCl is also observed in the case of the Au electrode covered with a film of the (PBTh-Py)⁺AOT⁻/SWNTs composites (Fig. 6). In our opinion, these changes indicate an irreversible character in terms of insertion and expulsion of ClO₄⁻ anions in the matrix of the (PBTh-Py)⁺AOT⁻ copolymer and the (PBTh-Py)⁺AOT⁻/SWNTs composites. According to above results, the conducting properties of the Au electrodes covered with films of the (PBTh-Py)⁺AOT⁻ copolymer and the (PBTh-Py)⁺AOT⁻/SWNTs composite increase when: i) the electrolyte contains cations with large ionic radius; an increase in the current densities was evidenced in the case of cyclic voltammograms recorded on the electrodes immersed in the electrolyte solutions contains K⁺ ions in comparison with the Na⁺ and Li⁺ ions and ii) the concentration of the electrolyte solution increases. The oxidation and reduction reactions which take place at the interface of electrode/electrolyte, in the case of the (PBTh-Py)⁺AOT⁻ copolymer and the (PBTh-Py)⁺AOT⁻/SWNTs composite can be described by the following equations:



where X⁺ = Li⁺, Na⁺, K⁺ and Y⁻ = ClO₄⁻.

With all these in the mind, the assessing of the performances of supercapacitor cells having the (PBTh-Py)⁺AOT⁻ copolymer and the (PBTh-Py)⁺AOT⁻/SWNTs composite as electrode active materials and the 1M LiPF₆ solution as electrolyte were carried out by cyclic voltammetry studies and the charge-discharge galvanostatic tests. According to Fig. 7, cyclic voltammograms recorded using cells assembled with electrodes containing as active material the (PBTh-Py)⁺AOT⁻ copolymer and an electrolyte of the type the 1M LiPF₆ solution are characterized after the 200th cycle by the anodic and cathodic peaks situated at the potentials of +0.04 V and -0.09 V, respectively.

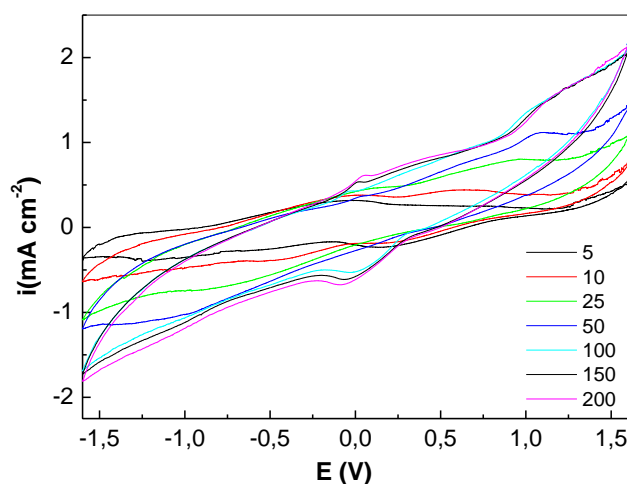


Figure 7. Cyclic voltammograms of symmetric supercapacitors having as active material of the (PBTh-Py)⁺AOT⁻ copolymer, recorded after 5, 10, 25, 50, 100, 150 and 200 cycles performed in the potential range (-1.6; +1.6) V with a sweep rate 100 mV s⁻¹.

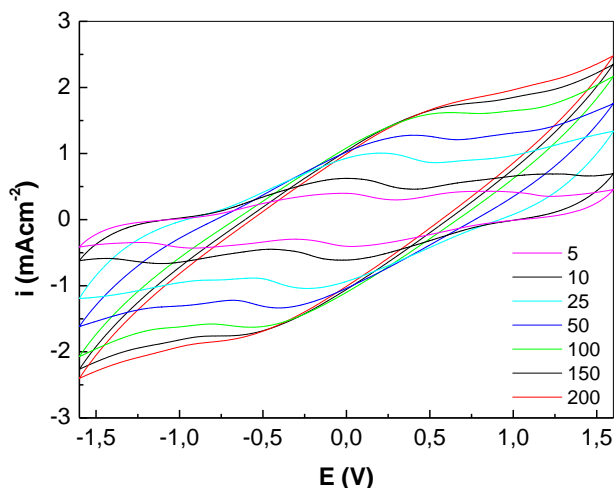


Figure 8. Cyclic voltammograms of symmetric supercapacitors having as active material of the $(\text{PBTh-Py})^+\text{AOT}^-/\text{SWNTs}$ composite, recorded after 5, 10, 25, 50, 100, 150 and 200 cycles performed in the potential range (-1.6; +1.6) V with a sweep rate 100 mV s^{-1} .

The profile of the cyclic voltammetry, shown in Fig. 7, indicates an additional double-layer contribution to the faradaic process. In the case of the $(\text{PBTh-Py})^+\text{AOT}^-/\text{SWNTs}$ composite, the cyclic voltammograms shown in Fig. 8 have a rectangular profile which is characteristic of electrical double layer which is not accompanied by a faradaic process. In addition, the current densities in the case of the cyclic voltammograms recorded using electrodes based on the $(\text{PBTh-Py})^+\text{AOT}^-/\text{SWNTs}$ composite are superior to those recorded when electrodes contain the $(\text{PBTh-Py})^+\text{AOT}^-$ copolymer as active material. This fact is a consequence of the formation of an electrical network as a result of SWNTs presence in the composite mass. [13] These results allow to anticipate higher values of capacitance for the electrodes that contains the $(\text{PBTh-Py})^+\text{AOT}^-/\text{SWNTs}$ composite in comparison with the electrodes having the $(\text{PBTh-Py})^+\text{AOT}^-$ copolymer as active material. Fig. 9 confirms this foresight.

In this stage of our studies, it is important to notice a decrease of capacitance in the first 150 charge-discharge cycles when supercapacitor cells have the $(\text{PBTh-Py})^+\text{AOT}^-$ copolymer as the electrode active material (Fig. 9a). A decrease of capacitance in the first 110 charge-discharge cycles is also noted in the case of the supercapacitor cells which have the $(\text{PBTh-Py})^+\text{AOT}^-/\text{SWNTs}$ composite as the electrode active material (Fig. 9b). These decreases in the specific capacitance are often correlated in supercapacitors field with the porous structure of the active material, the diffusion being the determinant stage at high values of current densities when the formation of electric double-layer on the electrode surface takes place. By analogy with Ref. [9], these changes can be explained considering expansion and contraction the electrode volume due of the ions insertion and expulsion when it is induced a stress of active material of electrode and its interface. These processes can be described by the following reactions:



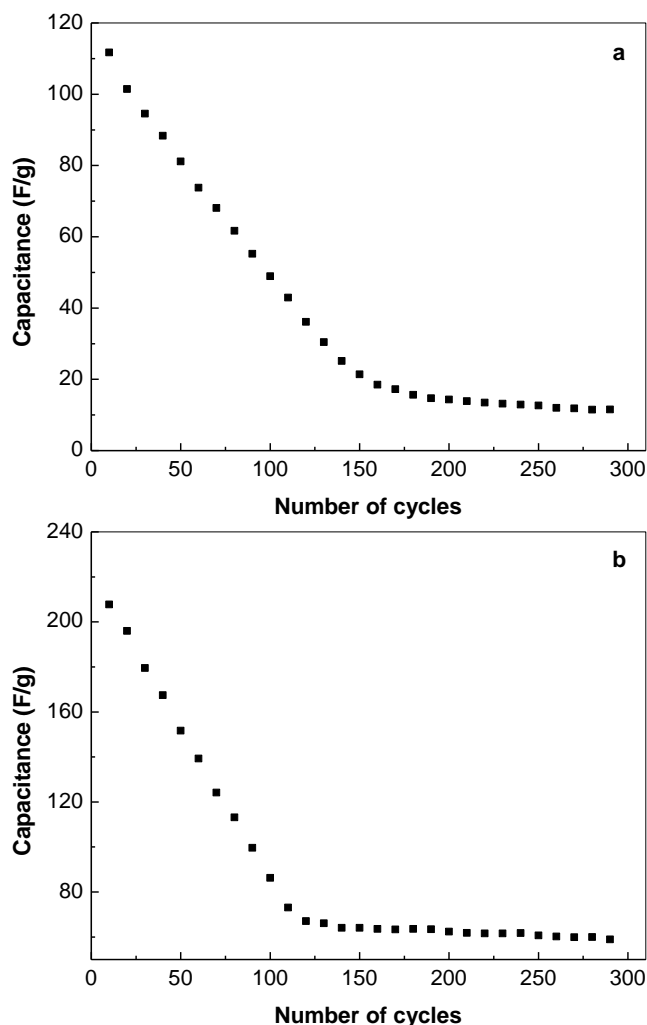


Figure 9. The evolution of the capacitance of symmetrical supercapacitors having the (PBTh-Py)⁺AOT⁻ copolymer (a) and the (PBTh-Py)⁺AOT⁻/SWNTs composite (b) as electrode active material during the successive 300 charge-discharge cycles, recorded at the current density of 100 mA g⁻¹.

The above reactions show that in the first discharge half-cycle, the AOT⁻ ions leave the (PBTh-Py)⁺AOT⁻/SWNT composite matrix while in the first charge half-cycle the interaction of the (PBTh-Py)/SWNTs composite both with the AOT⁻ and PF₆⁻ ions occurs. Taking into account that the volume of PF₆⁻ ions is smaller than the volume of AOT⁻ ions, as increasing of the charge-discharge cycles number a progressive replacement of AOT⁻ ions with the PF₆⁻ ions takes place. This fact is illustrated in Figs. 9a and 9b by a significant decrease of the capacitance in the two cases. After the 150th charge-discharge cycle, only small variations are observed in Figs. 9a and 9b; after the recording of the 300th charge-discharge cycle, at the current density of 100 mA g⁻¹ in the case of symmetrical supercapacitors having the (PBTh-Py)⁺AOT⁻ copolymer and the (PBTh-Py)⁺AOT⁻/SWNTs composite, the capacitance

values of ~ 11.5 and 59 F g^{-1} , respectively, are reported. These results demonstrate clearly that the $(\text{PBTh-Py})^+\text{AOT}^-/\text{SWNTs}$ composite can be used successfully as electrode active materials in symmetrical supercapacitor cells. However, a careful analysis of the capacitance values reported in the case of galvanostatic charge-discharge measurements of the symmetrical or non-symmetrical supercapacitors assembled using the conjugated polymers/carbon nanotubes composites as electrodes active materials and Li salts as electrolytes (Table 1) indicates that an improvement of the performances of supercapacitors having the $(\text{PBTh-Py})^+\text{AOT}^-/\text{SWNTs}$ composite based electrodes, by the changing the active material weight in the electrode mass as well as electrolyte, is necessary to be carried out in the next period. Taking into account that as increasing current density, a decrease in the capacitance value of supercapacitors takes place, we conclude that the capacitance values of the symmetrical supercapacitors having electrodes based on the $(\text{PBTh-Py})^+\text{AOT}^-/\text{SWNTs}$ composite are higher to those reported in the case of the non-symmetrical supercapacitors shown in Table 1 [18] and smaller to those of symmetrical supercapacitors having the PVK/SWNTs and PEDOT-MWNTs composites as electrode active materials. [19, 20]

Table 1. The value of the capacitance of the symmetrical or non-symmetrical supercapacitors

Electrodes with different active materials*	Electrolyte concentration	Current density (mA g^{-1})	Capacitance (F g^{-1})	Reference
MWNTs-PPY/MWNTs-PMeT	1M LiClO_4 in CH_3CN	1	87	[18]
MWNTs/MWNTs-PMeT	1M LiClO_4 in CH_3CN	1	45	[18]
MWNTs/MWNTs-PPY	1M LiClO_4 in CH_3CN	1	72	[18]
PVK-SWNTs/PVK-SWNTs	1M LiPF_6 in EC:DMC	100	92.27	[19]
PEDOT-MWNTs/PEDOT-MWNTs	1M LiClO_4 in CH_3CN	500	81	[20]

*MWNTs = multi-walled carbon nanotubes, PPY = polypyrrole, PMeT = poly(3-methylthiophene), PVK = poly(N-vinylcarbazole), PEDOT = poly(3, 4-ethylenedioxythiophene).

4. CONCLUSIONS

In this work, new electrochemical properties of the $(\text{PBTh-Py})^+\text{AOT}^-$ copolymer and the $(\text{PBTh-Py})^+\text{AOT}^-/\text{SWNTs}$ composite are reported.

Using cyclic voltammetry we have shown that the dependence of electrochemical properties of the $(\text{PBTh-Py})^+\text{AOT}^-$ copolymer and the $(\text{PBTh-Py})^+\text{AOT}^-/\text{SWNTs}$ composite, as function of the concentration and the cations type of the electrolyte solution, on the oxidation and reduction reactions at the electrolyte/electrode interface can be explained taking into account the diffusion processes of the cations and anions from and into the copolymer or composite matrix.

The charge-discharge galvanostatic measurements have indicated that in the case of the symmetrical-supercapacitors having as electrode active materials, the (PBTh-Py)⁺AOT⁻ copolymer and the (PBTh-Py)⁺AOT⁻/SWNTs composite, values of the specific capacitance equal with 11.5 and 59 F g⁻¹, respectively, for current densities of 100 mA g⁻¹ after 300 charge-discharge cycles were obtained.

ACKNOWLEDGMENTS

Part of this work was funded by the Romanian National Authority for Scientific Research, CNCS-UEFISCDI, the PN-II-ID-PCE-2011-3-0623 project.

References

1. I. Smaranda, M. Baibarac, M. Ilie, A. Matea, I. Baltog and S. Lefrant, *Curr. Org. Chem.*, 19 (2015) 652.
2. M. Baibarac, I. Baltog, I. Smaranda, M. Scocioreanu, J. Y. Mevellec and S. Lefrant, *Appl. Surf. Sci.*, 302 (2014) 11.
3. A. Q. Zhang, L. Z. Wang, L. S. Zhang and Y. Zhang, *J. Appl. Polym. Sci.*, 115 (2010) 1881.
4. B. Yue, C. Wang, P. Wagner, Y. Yang, V. Ding, D. L. Officer and G. G. Wallace, *Synth. Met.*, 162 (2012) 2216.
5. M. Gholami, P. M. Nia, L. Narimani, M. Sokhakian and Y. Alias, *Appl. Surf. Sci.*, 378 (2016) 259.
6. B. Liang, Z. Qin, T. Li, Z. Dou, F. Zeng, Y. Cai, M. Zhu and Z. Zhou, *Electrochim. Acta*, 177 (2015) 335.
7. M. Baibarac, I. Baltog, S. Frunza, A. Magrez, D. Schur and S. Yu Zaganaichenko, *Diamond Rel. Mater.*, 32 (2013) 72.
8. J. M. Pernant, R. C. D. Peres, V. F. Juliano and M. A. de Paoli, *J. Electroanal. Chem.*, 274, (1989) 225.
9. G. Bidan, E. M. Genies and M. Lapkowski, *J. Electroanal. Chem.*, 259 (1988) 297.
10. V. Haase and F. Beck, *Electrochim. Acta*, 39 (1994) 1195.
11. R. C. D. Peres, J. M. Pernant and M. A. De Paoli, *Synth. Met.*, 28 (1989) 59.
12. M. A. de Paoli, S. Panero, S. Passerini and B. Scrosati, *Adv. Mater.*, 2 (1990) 480.
13. V. Branzoi, L. Pilan and F. Branzoi, *Electroanalysis*, 21 (2009) 557.
14. C. Fu, H. Zhou, R. Liu, R. Huang, J. Chen and Y. Kuang, *Mat. Chem. Phys.*, 132 (2012) 596.
15. V. Bavastrello, S. Carrara, M. K. Ram and C. Nicolini, *Langmuir*, 20 (2004) 969.
16. B. Sljukic, C. E. Banks, C. Salter, A. Crossley and R. G. Compton, *Analyst*, 131 (2006) 670.
17. M. Baibarac, I. Baltog, M. Scocioreanu, S. Lefrant and J. Y. Mevellec, *Synth. Met.*, 159 (2009) 2550.
18. Q. Xiao and X. Zhou, *Electrochim. Acta*, 48 (2003) 575.
19. M. Baibarac, P. Gomez-Romero, M. Lira-Cantu, N. Casan-Pastor, N. Mestres and S. Lefrant, *Eur. Polym. J.*, 42 (2006) 2302.
20. X. Bai, X. Hu, S. Zhou, J. Yan, C. Sun, P. Chen and L. Li, *Electrochim. Acta*, 87 (2013) 394.

© 2017 The Authors. Published by ESG (www.electrochemsci.org). This article is an open access article distributed under the terms and conditions of the Creative Commons Attribution license (<http://creativecommons.org/licenses/by/4.0/>).